Transport properties between quantum Hall plateaus

Dmitri B. Chklovskii and Patrick A. Lee
Department of Physics, Massachusetts Institute of Technology, Cambridge, Massachusetts 02139
(Received 9 April 1993; revised manuscript received 8 July 1993)

We propose a unified transport theory for the two-dimensional electron gas in the dissipative quantum Hall regime in the presence of a long-range disorder. We find that the evolution of the longitudinal conductivity peaks as a function of the disorder can be described by a single parameter β^{-1} which is determined by the typical gradient of the electron-density fluctuations. In the case of a relatively strong disorder we utilize the edge-states-network model to describe transport in a half-filled Landau level. In the fractional quantum Hall regime we apply the network model to the system of composite fermions, finding the universal values of the resistivity at even-denominator filling fractions. The breakdown of the network model takes place at weak disorder because the edge channels develop into wide compressible strips and at strong disorder because of the destruction of the incompressible strips, isolating the edge channels. We find the limits of the applicability of the network model in terms of β. In the limit of very weak disorder the system is effectively a Fermi liquid of composite fermions. We calculate the conductivity in this regime by considering the motion of noninteracting fermions in a spatially varying magnetic field arising from the density fluctuations. The resistivity is found to scale linearly with the magnetic field with the slope given by β^{-1}. Although the presence of nonlocal transport makes measurements of the resistivity difficult, we find qualitative and, in some cases, quantitative agreement with experiment.

I. INTRODUCTION

The main features of the integer[1] and fractional[2] quantum Hall effects are the quantization of the Hall conductance and the vanishing of the longitudinal resistivity at integer and fractional filling factors correspondingly. The two discoveries generated an enormous amount of activity which resulted in significant progress in understanding of the properties of the two-dimensional electron gas (2DEG) in a strong magnetic field.[3] From a theoretical point of view the conductance quantization was understood in terms of the Landau quantization for integer filling factors and in terms of the formation of the incompressible liquid[4] for the fractional filling fac-

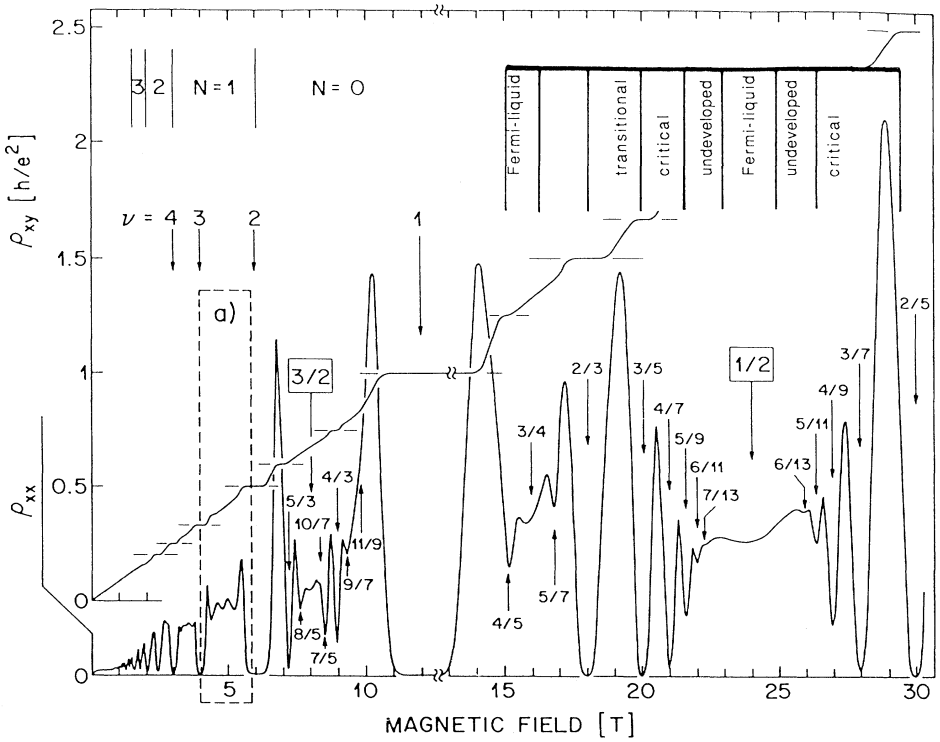

FIG. 1. ρ_{xx} and ρ_{xy} as a function of the magnetic field in a very high-mobility heterostructure. [Source: Willett *et al.* (Ref. 53)]. We have added labels to indicate our diagnosis of the principal sequence peaks. Note that the scale is reduced by the factor 2.5 for magnetic fields higher than 12 T.

tors. The exact quantization of the transport coefficients follows from the "gauge argument".[5]

Until recently, little attention was given to the dissipative regime, which is characterized by an unquantized Hall conductance and a finite longitudinal resistivity. A brief look at experimental data, Fig. 1, reveals an extraordinary diversity of the observed longitudinal resistivity values, which seem to vary from sample to sample.[6] Recently a significant effort was devoted to providing some theoretical basis for the dissipative regime. There are several approaches to this problem including the network model,[7,8] the law of corresponding states,[9,10] and the Fermi-liquid description.[11,12] However, it is not clear what the relationship between these theories is and whether they can explain the diversity in experimental data.

The purpose of this paper is to incorporate these approaches into a single picture, in which the relationship between various regimes is determined by a single parameter reflecting the level of disorder, and to find the longitudinal resistivity for different values of the parameter. We are able to do this for the case of high-mobility GaAs heterostructures where disorder is known to be of long-range nature: it comes from a nonuniform distribution of donors set back from the 2DEG plane by the spacer thickness d_s. Due to a very good screening by the 2DEG at zero magnetic field the long-range disorder potential is translated into electron density fluctuations. The characteristic length scale of these fluctuations is of the order of d_s, while the ratio of the average electron density, n_e, to the typical amplitude of the density fluctuations, δn_e, provides a natural large parameter β, on which our theory is based.

The value of β can be found approximately from the following consideration.[13,14] In an ungated heterostructure the concentration of ionized donors is equal to the electron concentration n_e. The number of ionized donors in a square with side d_s is equal to $n_e d_s^2$. The typical fluctuation in the number of donors is given by $(n_e d_s^2)^{1/2}$. This leads to the value of the relative density fluctuation

$$\beta = \frac{n_e}{\delta n_e} \sim \sqrt{n_e} d_s. \tag{1}$$

A more rigorous calculation of β yielding the numerical factor will be given in Sec. IV.

Our basic picture is that in a strong magnetic field, at a filling factor between the quantum Hall plateaus, the electron system breaks up into the incompressible regions corresponding to the integer or fractional states,[13,15] Fig. 2. Those regions are separated by edge channels which form a percolating network. Depending on the value of β these edge channels can be either wide or narrow. It turns out that the transport properties depend crucially on the width of the edge channels.

Although the longitudinal resistivity is measured at a fixed value of β with magnetic field being varied, it is enlightening to consider the evolution of resistivity between the quantum Hall plateaus with the variation of β. In the following we give a summary of the main results of this paper. For the sake of simplicity we consider the case of spinless electrons.

First, let us focus on the resistivity at a half-integer

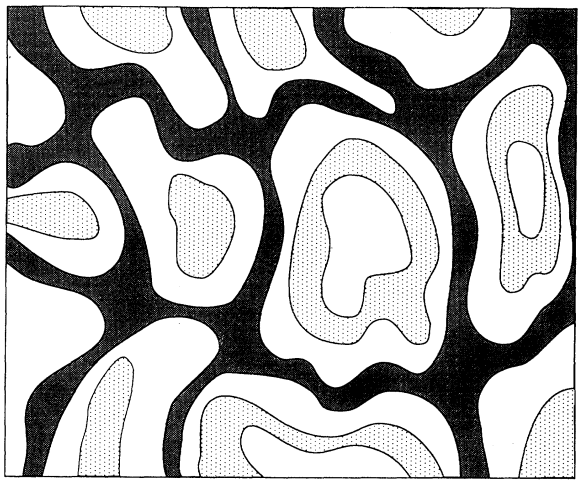

FIG. 2. Break-up of the electron system into the incompressible and compressible liquid regions. White regions represent incompressible liquid, while shaded regions correspond to compressible liquid: localized edge channels are dotted, extended channels are gray.

filling factor. In the case of a strong disorder (small β) a peak in longitudinal resistivity between the integer quantum Hall effect (IQHE) plateaus becomes infinitely sharp at low temperature. The related critical phenomena was studied extensively both theoretically and experimentally.[16] Thus we call this peak critical. In this case the edge states in the bulk of the sample (which we refer to as bulk edge states) are very narrow allowing us to describe them as one-dimensional channels comprised in a network. The transport properties of such a network have been considered in Refs. 7 and 8. Their result, derived using the Landauer formula as shown in Sec. III, states that the longitudinal conductivity of a half-filled Landau level is equal to $1/2(e^2/2\pi\hbar)$.

As β is increased the typical gradient of the electron density distribution at zero magnetic field becomes smaller and the bulk edge states acquire a finite width,[15,17–19] developing into the strips of compressible liquid. This leads to the breakdown of the network model and consequently to the reduction of the peak's height from its critical value. We call this peak "transitional" because it is about to give rise to the fractional states.

At larger values of β there is no well-defined peak at a half-integer filling factor. Rather one can see a slight depression in the longitudinal resistivity. The edge channel network disappears in this case because the compressible liquid occupies the whole plane. We believe that the proper description in this case is given by the Fermi liquid of composite fermions.[11,12]

Exactly at a half-integer filling factor the composite fermions do not experience any effective magnetic field on average. However, the variation of the filling factor leads to the appearance of the Shubnikov–de Haas oscillations which develop into the quantum Hall effect. Thus the principal sequence of the fractional quantum Hall effect (FQHE) is interpreted in terms of the IQHE for the composite fermions.[20] This interpretation allows us to explain the evolution of the longitudinal resistivity peaks

between the FQHE plateaus in analogy with the IQHE.

At sufficiently low disorder (large β) a peak in the longitudinal resistivity between the FQHE plateaus develops and becomes critical. The fractional edge channels in the bulk are very narrow. At even larger values of β the fractional peak becomes transitional because of the finite width of the bulk edge channels. This shows up in the reduction of the peak's height. As β is increased further, the peak starts giving rise to the daughter states of the next generation of fractions. Then a Fermi-liquid state develops at the filling factor where the center of the peak used to be.

By applying this picture to the successive generations of fractions one can see that in the limit of very low disorder all the even denominator fractional filling factors end up in the Fermi-liquid regime.

To summarize the discussion, the whole lifecycle (β playing the role of time) of a given resistivity peak consists of four periods. The development of the peak is characterized by the growth of the peak's height and the decrease in the resistivity at the adjacent odd-denominator fractions. Then the peak becomes critical making it infinitely narrow at zero temperature. In the next stage the peak is transitional, its height reduced. Then it starts to produce the daughter states while staying in the Fermi-liquid regime. At this stage it would be more correct to talk about the even-denominator fraction and its vicinity rather than about the peak.

Now we can go back to the experimentally relevant situation where the value of β is fixed for a given sample, Fig. 1. We will show in this paper that the effective measure of disorder is different from peak to peak or, in other words, the values of β determining transitions between various regimes for a given peak depends on the peak's filling factor. Because of this in Fig. 1 some peaks are undeveloped, while some are critical and some are transitional, a few have turned into a Fermi-liquid state.

We consider fractions of the principal sequence of the FQHE defined by the filling factor $\nu = p/(2p+1)$, where p is an integer. The corresponding resistivity peaks between fractions $p/(2p+1)$ and $(p-1)/(2p-1)$ fall into one of the following categories as shown in Fig. 1:

$$\begin{array}{ll} \text{transitional peaks} & \text{for } |p| < p_{c1}, \\ \text{critical peaks} & \text{for } p_{c1} < |p| < p_{c2}, \\ \text{undeveloped peaks} & \text{for } |p| > p_{c2}. \end{array} \tag{2}$$

In Sec. IV we find from electrostatic considerations the widths of compressible and incompressible strips as a function of β. This yields the following transition values separating different regimes:

$$p_{c1} \approx \sqrt{\frac{\beta}{2}}, \tag{3}$$

$$p_{c2} \approx \left(\frac{\beta}{2}\right)^{4/5}. \tag{4}$$

We find the values of the resistivity for the critical peaks in the principal sequence by utilizing the theory of composite fermions. We apply the edge-state-network model to the fermion system and find the resitivity at the principal sequence peaks between fractions $p/(2p+1)$ and $(p-1)/(2p-1)$:

$$\rho_{xx} = \frac{2\pi\hbar}{e^2}\frac{1}{2p^2-2p+1}, \quad \rho_{xy} = -\frac{2\pi\hbar}{e^2}\frac{4p^2-2p+1}{2p^2-2p+1}. \tag{5}$$

Our values are in agreement with the law of corresponding states.[9,10]

Finally, we address the question of the Fermi-liquid states resistivity. In the composite fermion picture we calculate the resistivity of those states by considering the motion of noninteracting fermions in a fluctuating fictitious magnetic field arising from the density fluctuations. We find that the snake states play an important role in the transport in this regime. Unable to solve exactly the problem for random magnetic field we introduce a model in which the magnetic field varies abruptly between the two values. In this case we can solve the problem by applying the network model to the system of snake states. We find a linear dependence of the resistivity on the magnetic field B:

$$\rho_{xx} = \frac{B}{\beta n_e e c}. \tag{6}$$

We argue that this result should hold in a realistic case of smooth fluctuations.

The outline of the paper is as follows. Section II is devoted to the discussion of the transition between narrow and wide edge channels from the electrostatics point of view. In Sec. III we review the network model and reproduce the derivation of the conductivity tensor for a half-filled Landau level. In Sec. IV we consider the long-range disorder and use the results of Sec. II to derive the limits of the applicability of the network model. We also derive there the universal values of the resistivity peaks in the FQHE by applying the network model to the fermion system. In Sec. V we calculate the resistivity in the Fermi-liquid states at half-integer filling factors. We also formulate a general statement regarding the conductivity of the network model. The generalization to the even-denominator fractions of the principal sequence is done in Sec. VI. We compare our results with experiment in Sec. VII. Our major conclusions are given in Sec. VIII.

II. THE STRUCTURE OF EDGE CHANNELS IN THE QHE

As discussed in the Introduction, long-range disorder in GaAs heterostructures creates electron-density fluctuations in the absence of a magnetic field. Upon application of a magnetic field corresponding to a filling factor halfway between quantum Hall plateaus, the electron system breaks up into the incompressible regions with densities given by the quantum Hall states,[13–15] Fig. 2. Edge channels form along the boundaries of those regions comprising a complicated network. We will address the transport properties of the system by considering this network in detail. In this section we analyze the general structure of edge channels because of its impact on the transport properties which will be discussed in Sec. IV.

In the conventional one-electron picture it is assumed that the Landau levels are bent adiabatically by the confining potential. The intersection of the Landau levels with the Fermi level determines the location of the edge states. The typical width of an edge state is of the order of the magnetic length, $l_H = (\hbar c/eB)^{1/2}$. The distance between adjacent edge states is determined by the steepness of the external potential. But in order for the adiabatic approximation to be valid the distance between the edge states should be greater than l_H. This implies that in the one-electron picture the distance between the edge states is greater than their width.

The effect of electron-electron interaction on the structure of the edge states has been considered by Beenakker[18] and Chang[19]. They have shown that the formation of the edge states can be viewed as the result of nonlinear screening of an external potential by the 2DEG. According to the theory of nonlinear screening proposed by Efros[14,15] the 2DEG breaks up into the alternating strips of compressible and incompressible liquid. The compressible liquid consists of the states lying at the Fermi level which makes it a strongly screening media. On the other hand the incompressible liquid is characterized by the absence of gapless excitations and therefore does not screen.

Chklovskii, Shklovskii, and Glazman[17] gave an analytic solution of the electrostatic problem involving edge states, which agreed with the independent calculation of Kane[21] and an estimate by Efros.[22] It was shown that in a typical external potential compressible strips are wider than the adjacent incompressible ones contrary to the conclusion of the one-electron model. The result of Ref. 17 holds provided the strip dimensions are greater than the semiconductor Bohr radius, which is about 100 Å in GaAs.

In this paper we will extend these considerations to include the opposite limit of narrow compressible strips. Although relevance of this limit to the integer edge states in GaAs heterostructures seems doubtful, it might be important for some other 2DEG confinement schemes. Also we will show that this limit is of major importance in the FQHE regime. Throughout this paper we discuss the transport properties determined by the percolating network of edge channels. As edge channels follow the lines of constant density we consider the density distribution in the vicinity of a percolating line of constant density. In order to study the structure of edge channels we approximate the zero magnetic field density distribution around this line by a linear expansion. The slope of the density distribution n' is determined by β. This is equivalent to having in the $z = 0$ plane a background positive charge density constant in the y direction and varying linearly along the x axis

$$n(x) = n_0 + n'x. \tag{7}$$

Then, in the absence of a magnetic field, the equilibrium electron concentration can be found from the solution with a constant electrochemical potential in the area occupied by electrons. If we neglect the finite screening radius of the 2DEG and look for a solution with a constant electrostatic potential then the electron density distribution is given by Eq. (7).

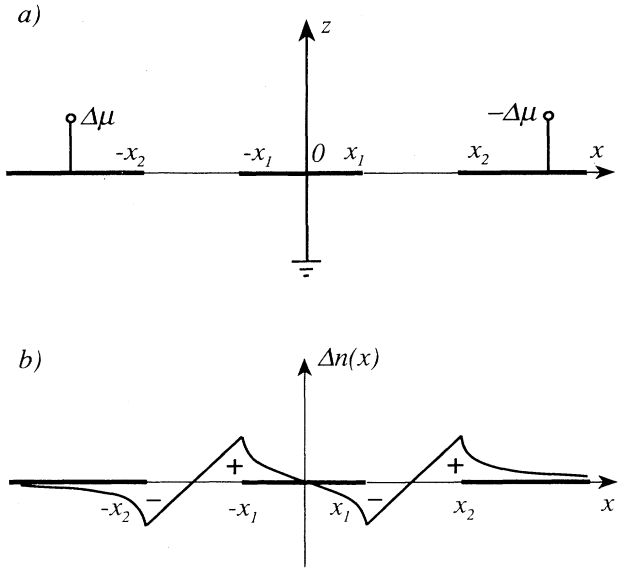

FIG. 3. (a) The formulation of the electrostatic problem for the two-gap model. Bold lines represent three metal planes. (b) Additional charge density distribution obtained by solving the electrostatics problem.

A strong magnetic field creates discontinuities in the chemical potential of the 2DEG at integer filling factors. This leads to the formation of the incompressible liquid strips across which the drop in the electrostatic potential occurs, which is needed in order to bring the next Landau level to the Fermi level. We adopt a two-gap model in which there are only two identical discontinuities in the chemical potential at the densities $n_0 - \Delta n/2$ and $n_0 + \Delta n/2$:

$$\mu = \begin{cases} -\Delta\mu, & n < n_0 - \Delta n/2, \\ 0, & n_0 - \Delta n/2 < n < n_0 + \Delta n/2, \\ \Delta\mu, & n > n_0 + \Delta n/2. \end{cases} \tag{8}$$

In order to find the charge distribution in this case we will treat the compressible regions as metal planes and the incompressible regions as insulators with fixed electron densities, Fig. 3. We allow the boundaries between the insulating and conducting regions, given by $\pm x_1, \pm x_2$, to vary. Thus we should solve the Laplace equation with mixed boundary conditions at the $z = 0$ plane. Electrostatic potential should be constant throughout each compressible strip

$$\phi(x, z = 0) = \begin{cases} \Delta\mu, & x < -x_2, \\ 0, & |x| < x_1, \\ -\Delta\mu, & x > x_2, \end{cases} \tag{9}$$

and the normal component of the electric field is given by the net charge density in each incompressible strip

$$E_z(x,z)|_{z\to -0} = \begin{cases} -\frac{2\pi e}{\epsilon}[n'x - (n_0 - \Delta n/2)], & -x_2 < x < -x_1, \\ -\frac{2\pi e}{\epsilon}[n'x - (n_0 + \Delta n/2)], & x_1 < x < x_2. \end{cases} \tag{10}$$

In order to ensure mechanical equilibrium at the boundaries of compressible and incompressible strips we set

$$E_x(x,0)|_{x\to -x_2+0} = E_x(x,0)|_{x\to -x_1-0} = E_x(x,0)|_{x\to x_1+0} = E_x(x,0)|_{x\to x_2-0} = 0. \tag{11}$$

This problem can be solved as shown in the Appendix by employing the methods of complex analysis. One gets the following system of equations determining the dimensions of the strips:

$$\begin{aligned} &\int_{x_1}^{x_2} dx \frac{(n'x-\Delta n/2)x^2}{\sqrt{(x_2^2-x^2)(x^2-x_1^2)}} = \frac{\epsilon\Delta\mu}{2\pi e^2}, \\ &\int_{x_1}^{x_2} dx \frac{n'x-\Delta n/2}{\sqrt{(x_2^2-x^2)(x^2-x_1^2)}} = 0. \end{aligned} \tag{12}$$

We solved this system of equations numerically. The position of the incompressible strip boundaries as a function of the inverse density gradient is plotted in Fig. 4. In the two limiting cases the system allows an approximate solution.

If the density gradient is small then the widths of the incompressible strips are much smaller than the distance between them, Fig. 5(a). Equations (12) are reduced to

$$\begin{aligned} &\int_{x_1}^{x_2} dx \frac{(n'x-\Delta n/2)x}{\sqrt{(x_2-x)(x-x_1)}} = \frac{\epsilon\Delta\mu}{2\pi e^2}, \\ &n'\tfrac{x_1+x_2}{2} - \Delta n/2 = 0. \end{aligned} \tag{13}$$

By solving this system of equations we find

$$(x_2 - x_1)^2 = \frac{4\epsilon\Delta\mu}{\pi^2 e^2 n'}, \tag{14}$$

$$\frac{x_1 + x_2}{2} = \frac{\Delta n}{2n'}. \tag{15}$$

These formulas describe two independent dipolar strips of Ref. 17.

When the density gradient is increased the two incompressible strips start to interfere with each other because their widths become comparable to the distance between them. In the extreme limit of a large density gradient the compressible strip is squashed by the incompressible ones, Fig. 5(b). Then Eqs. (12) are reduced to

$$\begin{aligned} &\int_{x_1}^{x_2} dx \frac{(n'x-\Delta n/2)x}{\sqrt{x_2^2-x^2}} = \frac{\epsilon\Delta\mu}{2\pi e^2}, \\ &n'\pi = \Delta n \int_{x_1}^{x_2} \frac{dx}{\sqrt{(x_2^2-x^2)(x^2-x_1^2)}}. \end{aligned} \tag{16}$$

By solving this equation we find

$$(2x_2)^2 = \frac{4 \times 2\epsilon\Delta\mu}{\pi^2 e^2 n'}, \tag{17}$$

$$x_1 = 4x_2 \exp\left(-\pi \frac{x_2 n'}{\Delta n}\right). \tag{18}$$

Equation (17) is just the old expression for the dipolar strip width[17] with the potential drop of $2\Delta\mu$.[23] But Eq. (18) is a new result showing that the width of the incompressible strip decreases exponentially fast with in-

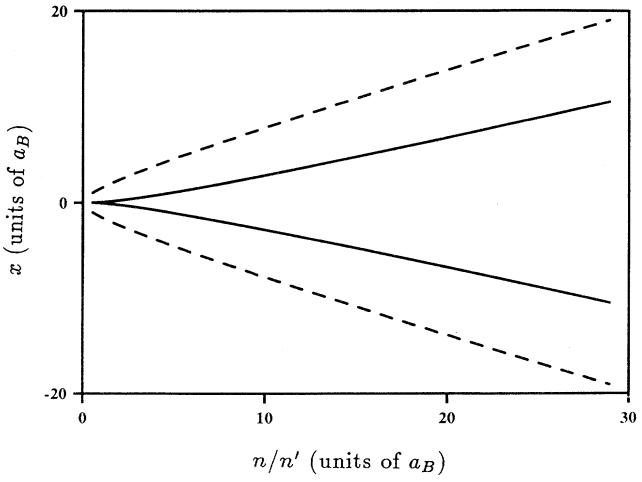

FIG. 4. The locations of the incompressible strip boundaries $\pm x_1, \pm x_2$ as a function of the inverse density gradient. The full lines show the inner boundaries of the incompressible strips and the dashed lines represent the outer boundaries.

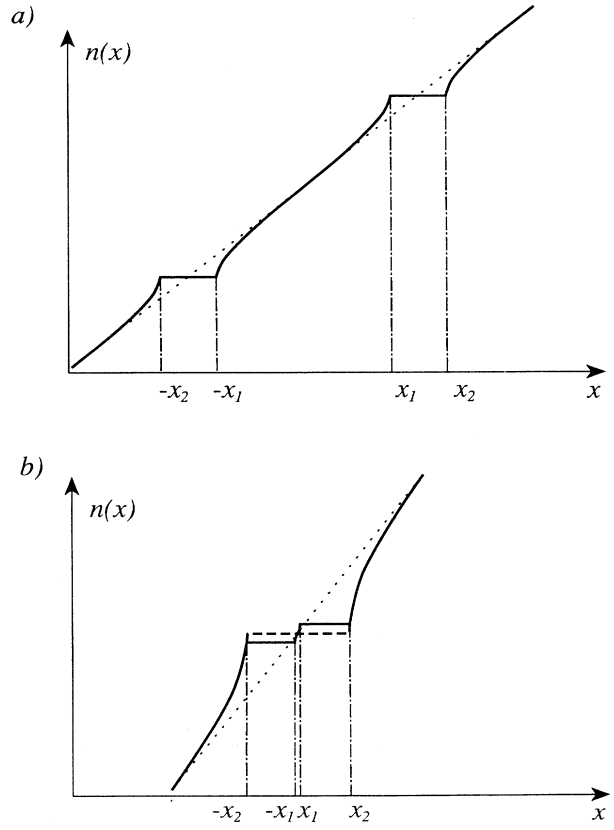

FIG. 5. The evolution of the electron density distribution with the changing density gradient in the two-gap model. The dotted line shows electron density at zero magnetic field. (a) The $a \ll b$ case, when the two dipolar strips are independent. (b) the $a \gg b$ case when the charge distribution can be thought of as a single dipolar strip (dashed line) plus two slabs with opposite charge.

creasing density gradient. A similar formula has been derived by Cooper and Chalker.[24]

Let us give a qualitative derivation of Eq. (18). When the incompressible strips are wide one can ignore the step in electron density between them [dashed line in Fig. 5(b)] and find x_2 from Eq. (17). The appearance of the compressible strip at $x = 0$ can be considered as a perturbation which does not affect the value of x_2. Thus we can view the formation of the compressible strip as a charge redistribution that screens out the electric field in the interval $|x| < x_1$ created by the dipolar strip extending from $-x_2$ to $+x_2$. This redistributed charge density consists of two slabs

$$en(x) = e\Delta n/2, \quad x_1 < x < x_2, \tag{19}$$

$$en(x) = -e\Delta n/2, \quad -x_2 < x < -x_1. \tag{20}$$

The electric field created by these slabs at $x = 0$ is given by

$$E_x = \int_{x_1}^{x_2} \frac{dx 2\Delta ne}{\epsilon x} = \frac{2\Delta ne}{\epsilon} \ln \frac{x_2}{x_1}. \tag{21}$$

By setting this field to be equal to the field in the middle of the unperturbed double dipolar strip[17] $E = 2\pi en' x_2/\epsilon$ we find

$$x_1 \approx x_2 \exp\left(-\pi \frac{x_2 n'}{\Delta n}\right) \tag{22}$$

in agreement with Eq. (18).

In the IQHE regime $\Delta n = n_L = 1/2\pi l_H^2$ and $\Delta\mu = \hbar\omega_c$. By substituting this in Eqs. (17) and (18) we find for the incompressible and compressible strips widths $a = x_2 - x_1$ and $b = 2x_1$

$$b = 8a \exp\left(-\frac{2\epsilon\hbar\omega_c}{a\pi e^2 n_L}\right) = 8a \exp\left(-\frac{4a_B}{a}\right)$$

$$\text{for } b \ll a \ll a_B, \tag{23}$$

where we have used the Bohr radius in semiconductor $a_B = \hbar^2\epsilon/m_{\text{eff}}e^2$. This should be contrasted with the result of Ref. 17 which can be recovered from Eqs. (14) and (15):

$$a^2 = \frac{8}{\pi} a_B b \text{ for } a_B \ll a \ll b. \tag{24}$$

We would like to point out that the applicability of Eqs. (18) and (23) for the 2DEG in GaAs heterostructures in the IQHE regime is very limited. It only shows that as soon as the gradient becomes high so that $a \approx b$ the compressible liquid strip starts shrinking exponentially fast. Naturally, when b is of the order of the magnetic length, a quantum mechanical consideration is necessary.

Now we extend our treatment to the FQHE regime. We consider first the fractions of the principal sequence with the filling factor of the form $p/2p + 1$, where p is either negative or positive integer. In the limit of large $|p|$ the sequence converges towards $1/2$ either from above or below depending on the sign of p.

The most dramatic prediction of the Fermi-liquid theory proposed by Halperin, Lee, and Read[11] is for the size of the energy gaps at filling factors $p/2p+1$. They claim that the discontinuities in the chemical potential at these filling factors should be independent of p. This prediction has been recently verified experimentally[25] through a measurement of the activation exponent for a series of filling factors. As we shall see, this result has important implications on the structure of edge channels in the FQHE regime.

We will use the experimental value for the chemical potential discontinuity found from the activation energy studies at the filling factor 1/3. According to Ref. 26 it is given by

$$\Delta\mu \approx 0.3 \frac{e^2}{\epsilon l_H}. \tag{25}$$

The difference in density between the adjacent filling factors $(p-1)/(2p-1)$ and $p/(2p+1)$ is given by

$$\Delta n = \frac{n_L}{(2p+1)(2p-1)}. \tag{26}$$

By substituting this in Eqs. (17) and (18) we find

$$x_1 \approx 4x_2 \exp\left(-\frac{1.2(4p^2-1)l_H}{x_2}\right) \tag{27}$$

or in terms of compressible and incompressible strip widths a and b

$$b \approx 8a \exp\left(-\frac{4p^2 l_H}{a}\right) \quad \text{for } b \ll a \ll p^2 l_H \tag{28}$$

in the limit of large p. Similarly from Eqs. (14) and (15) we get

$$a^2 \approx 3p^2 l_H b \quad \text{for } p^2 l_H \ll a \ll b. \tag{29}$$

The regime described by Eq. (28) has a much better chance of being realized in practice for the fractional case as opposed to the integer case. This is because the closeness of the filling factors between the adjacent fractions of the principal sequence leads to the appearance of the p^2 factor in Eq. (28) while the chemical potential discontinuity is independent of p. In Sec. IV we shall see that the narrow compressible strip limit described by Eq. (28) is realized for a certain range of p values.

Next we note that the perfect screening model used in solving the electrostatics model does not take into account the negative screening radius of the compressible liquid.[14] In order to check the validity of our picture in this case we have performed a numerical minimization of the total energy including correlations by looking for a solution with a constant electrochemical potential. We chose the chemical potential to vary linearly as a function of the filling factor, the total drop between two fractions being equal to the chemical potential discontinuity. We find similar behavior as the perfect screening model, except that the compressible strip shrinks even faster than given by the Eq. (28). Thus the conclusion is similar to the one in the IQHE regime: the transition from a wide edge channel to a narrow one occurs at such value of the

density gradient that

$$a \approx b \approx 4p^2 l_H. \tag{30}$$

The above electrostatic consideration can be generalized to any fractional filling factor, provided the discontinuities in the chemical potential are known.

III. EDGE STATES NETWORK MODEL

It is believed that in high-mobility samples dissipation between the quantum Hall plateaus occurs only due to transport in the topmost partially-filled (Nth) Landau level. Transport in the other $N-1$ Landau levels is dissipationless because of the absence of gapless bulk excitations. This fact has been confirmed in several experiments on high-mobility GaAs heterostructures.[8,27] Therefore in order to make predictions on the value of the dissipative conductivity we study a partially-filled Landau level.

We assume that it is possible to describe conductance in the partially-filled topmost Landau level with a local resistivity tensor ρ^N. In order to make a connection with experimentally measured quantities such as resistances R_{xx} and R_{xy} it is necessary to take into account the contribution of the lower Landau levels. This is not a trivial problem because these Landau levels, being perturbed by the confining potential, form edge channels at the boundaries of a sample. Hence their contribution may be strongly nonlocal,[28–31] making it impossible to describe a sample conductivity by a local resistivity tensor.

Szafer *et al.*[8] have considered the interplay of the nonlocal and local transport effects in detail. They have shown that only in the extreme case of strong equilibration between the edge channels and the bulk can one introduce a conductivity tensor σ, related to the conductivity of the Nth Landau level by

$$\sigma_{xx} = \sigma^N_{xx}, \quad \sigma_{xy} = \sigma^N_{xy} + (N-1)\frac{e^2}{2\pi\hbar}. \tag{31}$$

We will continue our discussion in terms of σ^N and σ assuming that Eq. (31) holds.

Our results for σ^N should be valid also in the regime when there is a significant nonlocal contribution to conductance. However in order to interpret experimental measurements in this case one has to analyze the experimental geometry in the spirit of Ref. 8. An example of such an analysis can be found in a recent work by Komiyama and Nii.[32]

Throughout this paper we study the contribution to the resitivity from the long-range external potential arising from a nonuniform donor distribution in heterostructures. We ignore the short-range potential fluctuations and keep in mind the zero-temperature limit.

Shapiro[33] has studied the dissipative transport between the quantum Hall plateaus by considering one-electron trajectories in a random external potential in the bulk. He has calculated the scattering rate between different extended states, which leads to the longitudinal resistivity. Shapiro has shown that the conductance of the half-filled Landau level is of the order of $e^2/2\pi\hbar$ and is independent of the Landau level number. Unfortunately, the picture presented in Ref. 33 does not include electron-electron interaction.

In the presence of interactions the 2DEG breaks up into compressible and incompressible regions[13–15] as shown in Fig. 2. Compressible strips are nothing else but edge channels, whose conductance in units of $e^2/2\pi\hbar$ is given by the difference in filling factors of the incompressible liquids on both sides of the channels. This result holds even in the presence of interactions as pointed out by Beenakker[18] in the FQHE regime. Therefore we include electron-electron interaction in consideration by applying the concept of the bulk edge states. We give this seemingly absurd name to the states formed at the intersection of the Fermi level with the topmost Landau level which is perturbed by the random potential in the bulk. These edge states follow the equipotential lines forming a random network.

The description of the conductance in a partially-filled Landau level with the help of the edge states network has been proposed by Kucera and Streda.[7] In principle the bulk edge channels should form a complicated percolation network. The topology of the network is simplified in the Kucera-Streda model to a square array of current-carrying loops. These loops are linked by scattering barriers transmitting fraction t of the incident current and reflecting the rest $r = 1 - t$ back in the loop. In the mean-field spirit all the transmission coefficients t are taken to be identical. By applying the Landauer-Buttiker formalism[48] to this model, Kucera and Streda have found a conductivity tensor in terms of r and t, which in turn depend on the average filling factor.

The Kucera-Streda model does not include the effects of quantum interference which should become important away from the point $r = t = 1/2$ and lead to Anderson localization. Chalker and Coddington[34] have introduced and studied numerically a network model similar to the one of Ref. 7. They included interference effects and found the divergence of the localization length in this model only at $r = t = 1/2$. However the physical nature of this transition still remains unclear.

We adopt the Kucera-Streda network model for the Landau level exactly at filling factor 1/2, in which case $r = t = 1/2$. Because of its conceptual importance we give a derivation of the conductivity in this model following the prescription of Ref. 8.

Let us assume that it is possible to create a uniform electric field E_x in the 2DEG plane. This is equivalent to having a constant gradient of the Fermi level $\nabla\mu = eE_x$ as shown in Fig. 6(a). Local nonequilibrium currents can be found by considering a single square, Fig. 6(b). Because the system is spatially uniform the current density is given by

$$j_x = \frac{1}{2}\frac{e}{2\pi\hbar}\nabla\mu, \quad j_y = \frac{1}{2}\frac{e}{2\pi\hbar}\nabla\mu. \tag{32}$$

Thus the conductivity tensor has the form

$$\sigma^N_{xx} = \frac{1}{2}\frac{e^2}{2\pi\hbar}, \quad \sigma^N_{xy} = \frac{1}{2}\frac{e^2}{2\pi\hbar}, \tag{33}$$

which is a special case of the formulas given in Ref. 7.

By adding the contribution of the $N-1$ filled Landau levels according to Eq. (31) one gets the following conductivity tensor:

$$\sigma_{xx} = \frac{1}{2}\frac{e^2}{2\pi\hbar}, \quad \sigma_{xy} = \left(N - \frac{1}{2}\right)\frac{e^2}{2\pi\hbar}. \tag{34}$$

This implies that the value of σ_{xx} at the peak should be independent of the Landau level number or, in other words, $\rho_{xx}(N+1/2) \sim B^2$.

The same conductivity tensor has been found by Huo, Hetzel, and Bhatt,[35] who have performed a computer simulation of a system of noninteracting electrons on the first Landau level. Their results have been obtained for the case of the short-range disorder suggesting that the result of Eq. (34) can be more general than would follow from the above derivation.

It is a formidable task to extract the value of σ_{xx} from the experiments with Hall bars because of nonlocal transport through edge states,[8,28–31] nonuniform current distribution,[36] and the spin-splitting of the Landau levels, taking place at small N. However there is some evidence[37] that σ_{xx} is independent of N. The absolute value of the conductivity in Ref. 37 was in agreement with Eq. (34) although the observation was made for the spin-unresolved peaks. We believe that the use of Corbino geometry or noncontact measurements may help to verify the correctness of Eq. (33).

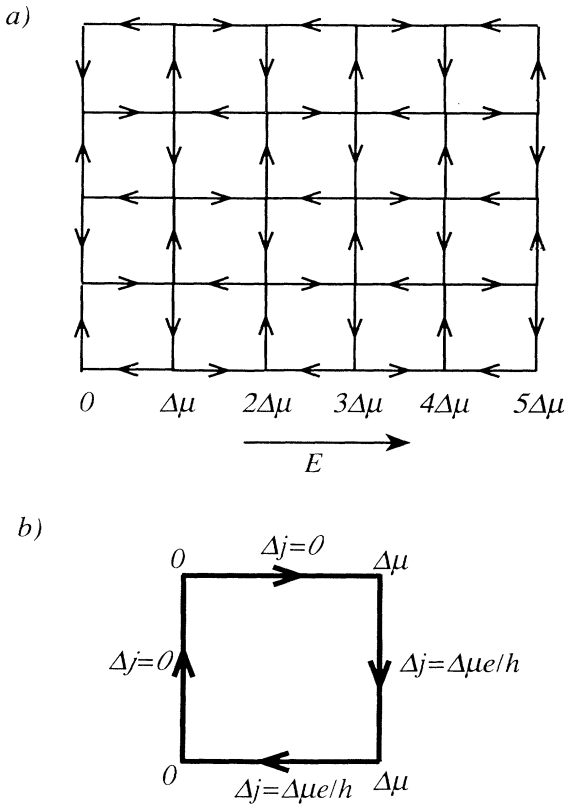

FIG. 6. (a) The simplified edge-states network. Arrows show the directions of propagation along each link. (b) Currents carried along the sides of a single square according to the Landauer formula.

An important assumption in the derivation of Eq. (34) was in describing scattering in the nodes of the network by a single scattering probability: only then can one assign a single value of the chemical potential to a node. The validity of this assumption depends crucially on the detailed structure of the bulk edge channels. In particular if the edge channels are wide the scattering of an electron may depend on its position across the channel. This situation will be discussed in terms of composite fermions in Sec.VI. The limit of extremely wide channels will be treated in the Fermi-liquid framework in Sec. V.

IV. EVOLUTION OF THE QHE IN SAMPLES WITH LONG-RANGE DISORDER

In the network model reviewed in Sec. III the conductivity of a half-filled Landau level is given by the universal value, Eq. (33). However, the experimental data exhibit a much richer behavior. Not only may the absolute values of the resistivity fluctuate, but also the peaks may not be infinitely sharp in the limit of zero temperature. In this section we discuss the limits of applicability of the network model relying on the results obtained in Sec. II.

We start by considering the IQHE regime although the quantitative results obtained for this case are likely to be incorrect because of the importance of the quantum effects. Then we treat the FQHE regime in the same spirit using the concept of composite fermions. We believe that our theory is actually more reliable than in the IQHE case, even though we find a certain disagreement with available data.

In high-mobility GaAs heterostructures, widely used to study transport properties of the 2DEG, the major contribution to disorder comes from the long-range potential due to the random distribution of ionized donors behind the spacer layer. For the sake of simplicity we consider the case of a noncorrelated donor distribution and assume that the average densities of ionized donors and electrons are identical. Then, following Refs. 38 we have for the deviation δn_i from the average ionized donor density n_i:

$$\langle \delta n_i(\mathbf{r}) \rangle = 0, \tag{35}$$

$$\langle \delta n_i(\mathbf{r}_1)\delta n_i(\mathbf{r}_2) \rangle = n_i \delta(\mathbf{r}_1 - \mathbf{r}_2), \tag{36}$$

where $\langle\,\rangle$ denotes a statistical average. By making Fourier transformation of Eq. (36) we find

$$\langle \delta n_i(\mathbf{q}_1)\delta n_i(\mathbf{q}_2) \rangle = (2\pi)^2 n_i \delta(\mathbf{q}_1 + \mathbf{q}_2). \tag{37}$$

As discussed in Ref. 38, because of screening by the 2DEG the deviation δn_e from the average electron density $n_e = n_i$ can be related to δn_i by

$$\delta n_e(\mathbf{q}) = \delta n_i(\mathbf{q}) \exp(-q d_s). \tag{38}$$

Then the mean square deviation in the electron density

$$\delta n_e = \frac{\sqrt{n_e/8\pi}}{d_s}. \tag{39}$$

Rewriting this in terms of the Fermi wave vector $k_F = \sqrt{4\pi n_e}$ we have

$$\delta n_e = \frac{n_e}{\sqrt{2}k_F d_s} = \frac{n_e}{\beta}. \quad (40)$$

Equation (40) defines the value of β in the case of the noncorrelated donor distribution. In typical high-mobility GaAs heterostructures $\beta \approx 10$–40 which makes it a natural large parameter.

It is quite possible that the distribution of ionized donors in heterostructures is correlated. In this case we can still introduce β as a typical relative electron density deviation. However Eq. (39) will not hold.

The typical density gradient can be found approximately from Eq. (40)

$$n' = \frac{\delta n_e}{d_s} = \frac{n_e}{\beta d_s}. \quad (41)$$

Now we can estimate the widths of compressible strips in the percolating network. As was done in Sec. II we approximate the density distribution by the linear expansion. Let us first consider the case of the IQHE. As discussed in Sec. II the small-gradient regime compressible strips are much wider than the incompressible ones. The typical width of the compressible strips in a strong magnetic field can be found from the condition

$$b = \frac{n_L}{n'}, \quad (42)$$

where $n_L = (2\pi l_H^2)^{-1}$ is the density in each Landau level. By expressing n_L in terms of the Landau level filling factor $N - 1/2$ and subsituting n' from Eq. (41) we find

$$b = \frac{\beta d_s}{N - 1/2}. \quad (43)$$

This formula is only valid when it yields b less than d_s, otherwise it indicates that all the 2DEG is in the compressible state. By equating b with the Bohr radius [as follows from Eqs. (23) and (24)] we can find N at which in a given sample the transition to the large-gradient regime takes place:

$$N_c \approx \frac{\beta d_s}{a_B}. \quad (44)$$

For the filling factor $N > N_c$ the sample should be in the large-gradient regime: the compressible strips are narrow and the incompressible ones are wide. Then the conduction in the topmost Landau level can be described by the network model, yielding conductivity at half-integer filling factors independent of the number of filled Landau levels. In this case the resistivity peaks should scale as B^2.

At $N < N_c$ the description of the conduction in the topmost Landau level with the network model becomes inadequate. This is because the compressible liquid strips are wide and cannot be described as a single channel at the intersections. An essential assumption of the network model that there is an equal chance for an electron at each intersection to scatter left or right breaks down. It is natural to assume that for a wide edge channel one can introduce a quantum number characterizing the location of an electron across the channel. Then the transmission matrix at an intersection will depend on this quantum number. In other words, electrons which are closer to the right-hand side of the channel are more likely to go right at an intersection, while the ones closer to the left-hand side are more likely to go left. We will see in Sec.VI that this argument can be made more specific by considering composite fermions.

It has been argued by several authors[15,39,24] that the compressible regions are wide in the IQHE regime, making risers between the quantum Hall plateaus rather wide. Experimentally, it seems that the risers are narrower than expected. This discrepancy has been attributed in Ref. 39 to the localization of the compressible liquid, still an unresolved question. In this paper we take the point of view that at experimentally available temperatures localization occurs only for narrow channels on the scales of several network cells.

Our derivation of Eq. (44) relied on the fact that the total energy of the electron system can be written in terms of the density distribution. In this sense it is a classical theory, with quantum mechanics entering only with the cyclotron gap. Thus the theory is only valid when all the dimensions of the strips are larger than the typical extent of the electron wave functions, which is given by the cyclotron radius $R_c^N \approx \sqrt{N} l_H$ on the Nth Landau level. One can see that for the typical values of parameters, N_c obtained from Eq. (44) is already outside of the validity region. Moreover, the cyclotron radius in this case is larger than d_s. A detailed quantum mechanical consideration is needed, a problem which remains unsolved.

Now we switch our attention to the FQHE regime, in which the above limitations turn out to be weaker and the described transition may actually be observed.

We focus on the series of fractions with the filling factor given by $p/(2p+1)$, where p is either negative or positive integer. By using Eq. (41) we find the width of the compressible strip between filling factors $(p-1)/(2p-1)$ and $p/(2p+1)$ under the assumption $p \gg 1$

$$b = \frac{n_L}{(2p+1)(2p-1)n'} \approx \frac{\beta d_s}{2p^2}. \quad (45)$$

In order to find the critical value p_{c1} at which there is a transition to the narrow edge channels we combine Eqs. (30), (40), and (45)

$$p_{c1} \approx \sqrt{\frac{\beta}{2}}. \quad (46)$$

One can see that at this value of p the width of the compressible strips b as given by Eq. (45) is of the order of d_s. Therefore we think that the numerical factor in Eq. (46) is unreliable.

Equation (46) yields the critical fraction $(p_{c1} - 1)/(2p_{c1} - 1)$ at which the edge channels become narrow and one can apply the network model for $|p| > p_{c1}$. However in the FQHE regime we cannot directly apply Eq. (34) because the Landauer-Buttiker formalism[48] used in its derivation was obtained for noninteracting electrons. We overcome this problem by transforming the 2DEG to the system of composite fermions. The fractional filling factor $p/(2p+1)$ corresponds to integer effective filling factor p for composite fermions. Consequently the fractional electron edge states correspond to the inte-

ger fermion edge states. Thus we can legitimately apply Eq. (34) to the fermion system.

We consider the 2DEG at a critical filling factor, when the edge channels between regions with filling factors $(p-1)/(2p-1)$ and $p/(2p+1)$ form a percolating network. The critical filling factor is given by the mean of the two fractions only in a special case when there are no regions with other filling factors in the system. In the general case, however, there may be regions with filling factors less than $(p-1)/(2p-1)$ and greater than $p/(2p+1)$, see Fig. 2. Thus we believe that the exact position of the peaks is not universal and may vary from sample to sample. This conclusion does not contradict the results of Ref. 40, where the position of the peaks was found to be described by $(2p-1)/(4p)$ rather than by the arithmetic mean of $(p-1)/(2p-1)$ and $p/(2p+1)$. The 2DEG with uniform density at filling factor $(2p-1)/(4p)$ corresponds to the fermion system at filling factor $p-1/2$. For convenience in the rest of the paper we will refer to the peaks by fractions of the kind $(2p-1)/(4p)$, although the exact peak position may be slightly different.

Straightforward application of Eq. (34) gives the following conductivity tensor for the system of fermions:

$$\sigma_{xx}^{f}=\frac{1}{2}\frac{e^2}{2\pi\hbar},\quad \sigma_{xy}^{f}=\left(p-\frac{1}{2}\right)\frac{e^2}{2\pi\hbar}. \tag{47}$$

In order to obtain the physical transport coefficients we follow the procedure outlined in Ref. 11. The first step is to invert the conductivity tensor in order to obtain the resistivity tensor. Then one should add the contribution coming from the Chern-Simons gauge field:

$$\rho_{xx}^{\mathrm{CS}}=0,\quad \rho_{xy}^{\mathrm{CS}}=-2\frac{2\pi\hbar}{e^2}. \tag{48}$$

This originates from the phase factor in the fermion-electron transformation. A nice qualitative motivation for the summation of the resistivity tensors is described by Zhang.[41] Eventually, we find the following resistivity values for the filling factor $(2p-1)/(4p)$:

$$\rho_{xx}=\frac{2\pi\hbar}{e^2}\frac{1}{2p^2-2p+1},\quad \rho_{xy}=-\frac{2\pi\hbar}{e^2}\frac{4p^2-2p+1}{2p^2-2p+1}. \tag{49}$$

For example, by substituting $p=2$ we find that at filling factor 3/8 the resistivity tensor is

$$\rho_{xx}=\frac{2\pi\hbar}{e^2}\frac{1}{5},\quad \rho_{xy}=-\frac{2\pi\hbar}{e^2}\frac{13}{5}, \tag{50}$$

or for $p=-3$ (filling factor 7/12):

$$\rho_{xx}=\frac{2\pi\hbar}{e^2}\frac{1}{25},\quad \rho_{xy}=-\frac{2\pi\hbar}{e^2}\frac{31}{25}. \tag{51}$$

By inverting the resistivity tensor we find that conductivity is given by

$$\sigma_{xx}=\frac{e^2}{2\pi\hbar}\frac{1}{2(4p^2+1)},\quad \sigma_{xy}=\frac{e^2}{2\pi\hbar}\frac{4p^2-2p+1}{2(4p^2+1)}. \tag{52}$$

These transport coefficients are identical to that previously obtained by Kivelson, Lee, and Zhang[10] who mapped the fractional filling factor system onto the dirty boson model and took the boson conductivity such that it yields the universal value (34) for the IQHE. Thus our results are in agreement with the law of corresponding states.[9,10]

An advantage of our approach is that having a definite model in mind which yields Eqs. (49) and (52) enables us to give the limits for the validity of these results. We believe that Eqs. (49) and (52) are valid under the condition $|p|>p_{c1}$ and describe the critical peaks, i.e., the ones whose width goes to zero in the zero temperature limit.

As was mentioned previously the network model breaks down when the compressible strips become wide which should happen at $p=p_{c1}$. We will explain the nature of this transition from the composite fermion point of view in Sec. VI. The values of the resistivity are reduced in this case and the peaks may exhibit some additional structure. We call these peaks "transitional" because they are about (as disorder is reduced further) to give rise to the daughter fractions. These fractions appear when the compressible strips are wide enough for the incompressible strips of the higher order fractions to form along them.

Having narrow compressible strips is a necessary but not a sufficient condition for the validity of the network model. Another condition is imposed by the requirement that there is no equilibration between the transport edge channels (forming the percolating network) and localized edge channels (forming closed loops) as shown in Fig. 2. The suppression of the equilibration takes place because of the exponential decay of the wave functions of the edge states inside the incompressible strips. Therefore the equilibration rate is very sensitive to the width of the incompressible strips. This phenomenon has been studied experimentally for the fractional edge states by Kouwenhoven *et al.*,[42] Wang and Goldman,[43] and Chang and Cunningham.[44] Electrostatics based theoretical interpretation[17] seems to be in reasonable agreement with the data of Ref. 42.

In the IQHE the characteristic length of the exponential decay of the edge state wave function is the magnetic length l_H. We think that in the FQHE regime the effective magnetic length for the composite fermions, l_H^f, plays a similar role. Therefore the critical width of the incompressible strips at which the transport edge channels are practically destroyed is equal to l_H^f. In the state with the filling factor $p/(2p+1)$ and electron magnetic length l_H the fermion magnetic length is given by

$$l_H^f=l_H\sqrt{2p+1}. \tag{53}$$

Hence the breakdown of the network model takes place when the typical incompressible strip width

$$a=l_H^f=l_H\sqrt{2p+1}. \tag{54}$$

It seems plausible that the same condition should determine the disappearance of the fractionally quantized Hall plateaus and zero longitudinal resistivity values. This is because plateau formation should be due to the existence of the percolating incompressible strip network.[13–15]

It is likely that Eq. (54) determines the narrowest possible incompressible strip meaning that there could be no energy gap for the strips of smaller widths.

The transition to the Fermi-liquid state can be determined from the following considerations. The typical width of the incompressible liquid strips in the state with the average filling factor $(2p-1)/4p$ ($|p| > p_{c1}$) can be found by recalling that the compressible strips are much more narrow than the incompressible ones. Then the width of the incompressible strips is given by

$$a = \frac{n_L}{(2p-1)(2p+1)n'} \approx \frac{\beta d_s}{2p^2}, \tag{55}$$

where we assumed that $p_{c2} \gg 1$. By using the minimum width of the incompressible strip as given by Eq. (54) and recalling Eq. (40) we find the transition value p_{c2},

$$p_{c2} \approx \left(\frac{\beta}{2}\right)^{4/5}. \tag{56}$$

Therefore the network model should be applicable in the interval $p_{c1} < |p| < p_{c2}$, where p_{c1} and p_{c2} are given by Eqs. (46) and (56). We caution the reader that the numerical factors in Eqs. (46) and (56) should not be taken seriously.

We believe that a proper description of the case $|p| > p_{c2}$ should be given in the framework of the Fermi-liquid theory developed in Ref. 11. We consider this regime in Sec. V.

So far we discussed only the principal sequence of the filling fractions $p/(2p+1)$. Our results can be easily extended to the sequence of fractions converging to any half-integer filling factor. The universal resistivity values (49) correspond in this case only to the topmost Landau level. In other words Eq. (52) gives the values of σ_{xx}^N and σ_{xy}^N which are related to the experimentally observed transport coefficients as discussed in Sec. III.

V. TRANSPORT IN THE FERMI-LIQUID REGIME

In a recent paper[11] Halperin, Lee, and Read have suggested that a 2D system of strongly interacting electrons with Landau level filling factor 1/2 can be transformed to an equivalent system of fermions interacting with a Chern-Simons gauge field, such that the average effective magnetic field seen by fermions is zero. They have argued that even though the gauge field fluctuations lead to divergent corrections to the quasiparticle propagator the Fermi-liquid description of the fermion system is valid. The gauge transformation can also be performed[11] for the system of electrons with the filling factor $N-1/2$ by attaching two flux quanta only to the electrons on the topmost Landau level. In order to calculate the conductivity of such a system one needs to take disorder into account. As was done in Sec. IV we consider the case of the long-range disorder caused by a random distribution of ionized donors in GaAs heterostructures. At zero magnetic field the small angle scattering on this potential accounts for the zero temperature resistivity.

One can look at this mechanism from a different point of view. Due to a very strong screening by the 2DEG (screening radius equal to a_B) the long-range potential created by donors is transformed into the electron density fluctuations. Electrons are scattered by the density nonuniformities in a way similar to the propagation of light in a media with the varying index of refraction. The same mechanism exists for the system of fermions because fluctuations in the local densities of fermions and electrons are identical.

However it was argued in Refs. 11 and 12 that another scattering mechanism is important in a strong magnetic field. Due to the density fluctuations of the electron system fermions experience an effective fluctuating in space magnetic field. Scattering on this magnetic field accounts for a high resistivity at filling factors $N-1/2$. The amplitude of the effective magnetic field fluctuations is proportional to the density fluctuations of the electron system and the lengthscale of the fluctuations is equal to the spacer layer thickness d_s.

Halperin, Lee, and Read[11] have calculated the conductivity of the fermion system using Born approximation which is valid in the regime when $R_c^f \gg d_s$ (where R_c^f is the fermion cyclotron radius in the effective magnetic field) so that small-angle scattering by the magnetic field fluctuations is dominant. They found that the longitudinal resistance of the electron system is determined by the large parameter $k_F d_s$ and scales as the square root of the magnetic field. However, it seems that, experimentally, resistance at half-integer filling factors in the Fermi-liquid regime scales linearly[45,46] with the magnetic field. Halperin, Lee, and Read[11] argued that the discrepancy is due to the fact that except for $N=1$, the opposite limit $R_c^f \ll d_s$ is more appropriate so that Born approximation is not valid. In this section we calculate the conductivity in this limit.

Let us give an estimate of the effective magnetic field seen by the fermions following Ref. 11. The typical magnetic field can be found from the typical density fluctuation given by Eq. (40), recalling that each fermion carries two flux quanta:

$$\Delta B = 2\frac{2\pi\hbar c}{e}\delta n_e = 2\frac{2\pi\hbar c}{e}\frac{n_e}{\beta}. \tag{57}$$

The fermion cyclotron radius in the typical magnetic field ΔB can be found by expressing it in terms of the Fermi velocity v_F^f and the cyclotron frequency ω_c:

$$R_c^f = \frac{v_F^f}{\omega_c} = \frac{\hbar k_F^f}{e\Delta B/c}. \tag{58}$$

Substituting expression for ΔB and rewriting k_F^f in terms of the fermion concentration n_f one gets

$$R_c^f = d_s\sqrt{2\frac{n_f}{n_e}}. \tag{59}$$

The density of fermions coincides with the electron density only at filling factor 1/2. At filling factor $N-1/2$ the fermion density

$$n_f = \frac{n_e}{2N-1} \tag{60}$$

because only sitting on the topmost Landau level electrons are transformed into fermions. Substituting this in Eq. (59) one finds

$$R_c^f = d_s/\sqrt{N-1/2}. \tag{61}$$

Thus we find that the fermion cyclotron radius in the typical effective magnetic field is smaller than the length scale of the magnetic field fluctuations for large N.

It is clear that the conductance in this situation is determined mainly by the fermions that live near the lines of zero effective magnetic field because their cyclotron radius is large. Fermions that live in the areas of strong magnetic field drift slowly along the closed orbits and do not contribute much to the conductance of the system.

We will adopt a simplified model of the effective magnetic field fluctuations. Instead of considering a slowly varying magnetic field we will consider the case when the magnetic field takes only two values ΔB. Thus the whole plane is divided into areas of the typical size d_s where magnetic field has the same magnitude but randomly varying sign.

To calculate the conductance of such a system let us first solve a simpler problem. Let us consider the case when the magnetic field is translationally invariant along the x axis and is given by

$$B_z = \Delta B \mathrm{sgn}(y). \tag{62}$$

The one-particle Hamiltonian in Landau gauge with the magnetic field described by Eq. (62) is given by

$$H = \frac{1}{2m}\left[p_y^2 + \left(p_x - \frac{e\Delta B}{c}|y|\right)^2\right], \tag{63}$$

where p_x and p_y are the components of the momentum. The eigenfunctions of this Hamiltonian can be written in the form

$$\psi = \phi(p_x, y)\exp\left(i\frac{p_x}{\hbar}x\right), \tag{64}$$

where $\phi(p_x, y)$ is found by solving the equation

$$\frac{d^2\phi}{dy^2} + \frac{2m}{\hbar^2}(E - U_{\mathrm{eff}})\phi = 0 \tag{65}$$

with the effective potential, see Fig. 7:

$$U_{\mathrm{eff}} = \frac{1}{2m}\left(p_x - \frac{e\Delta B}{2c}|y|\right)^2. \tag{66}$$

Equation (65) can be solved quasiclassically. The spectrum is shown in Fig. 8. One can see that at large positive p_x the eigenvalues are doubly degenerate. They correspond to the eigenstates in a uniform magnetic field centered at $y = \pm p_x$. The total number of states is equal $2N_f$, where N_f is the number of filled Landau levels for fermions in the magnetic field ΔB:

$$N_f = \frac{2\pi\hbar c n_f}{e\Delta B}. \tag{67}$$

At smaller p_x the degeneracy is lifted and the states acquire velocity in the x direction. There is an interval of p_x where the velocity direction is reversed. The corresponding depression of the levels is small and therefore will be ignored. In order to discuss transport properties we focus on the states at the Fermi level. They are localized near the line $y = 0$ and have a velocity in the x direction. These states are called the snake states due to the characteristic shape of the classical analogue trajectories. As at $p_x \to -\infty$ all the eigenstates are above the Fermi level the total number of the snake states is $2N_f$. The snake states are reminiscent of the edge states in that they have a single velocity direction. The snake states, however, are all centered at $y = 0$ and are not spatially separated like the edge states.

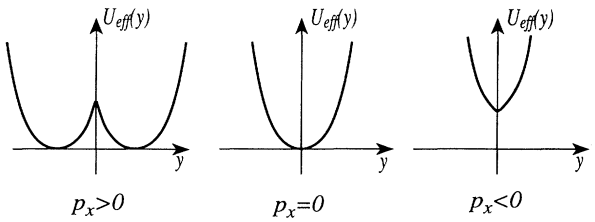

FIG. 7. Effective potential at different values of p_x.

The conductance of the fermion system along the line $y = 0$ can be found by using the Landauer formula,[48]

$$g = 2N_f\frac{e^2}{2\pi\hbar}. \tag{68}$$

Going back to the original problem with the magnetic field of varying sign we immediately notice that the snake states form a network very similar to the one considered for the edge states in Sec. III and shown in Fig. 6. This allows us to calculate the conductivity of the fermion system using the line of argument that led to Eq. (33):

$$\sigma_{xx}^f = g/2 = N_f\frac{e^2}{2\pi\hbar}, \quad \sigma_{xy}^f = 0. \tag{69}$$

Of course an important assumption made in the derivation of Eq. (69) was that the cyclotron radius for the topmost Landau level is smaller than the scale of the network.

We would like to formulate now a general statement, of which Eqs. (33) and (69) are the special cases. Suppose, one has a system of noninteracting fermions confined in a plane and subject to a perpendicular nonuniform magnetic field and some external potential. Suppose that the distribution of the magnetic field and external potential is such that the plane is broken up into the alternating regions with two filling factors

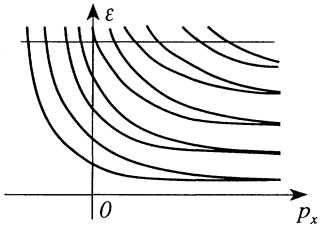

FIG. 8. Qualitative spectrum of the free-particle Hamiltonian with the steplike magnetic field. The double degeneracy at $p_x \to \infty$ represents Landau states to the right and to the left from $y = 0$.

$$N_1 = \frac{2\pi\hbar c n_1}{eB_1}, \quad N_2 = \frac{2\pi\hbar c n_2}{eB_2}, \tag{70}$$

where n_1,n_2 are densities and B_1,B_2 the magnetic fields. We assume that the Fermi level lies in the cyclotron gap inside the regions, henceforth N_1 and N_2 can be positive or negative integers . Then the system can be represented by a network of edge or snake channels. By using the Landauer approach we find the conductivity tensor to be

$$\sigma_{xx} = \frac{|N_1 - N_2|}{2}\frac{e^2}{2\pi\hbar}, \quad \sigma_{xy} = \frac{N_1 + N_2}{2}\frac{e^2}{2\pi\hbar}. \tag{71}$$

One can see that when $N_1 = N$, $N_2 = N - 1$ Eq. (71) is reduced to Eq. (34), and when $N_1 = -N_2 = N_f$ Eq. (71) is reduced to Eq. (69).

The general result, Eq. (71), allows for an accurate calculation of the resistivity at filling factor $N - 1/2$ (in the sharp-step model). The typical magnetic field seen by fermions is given by Eq. (57), and the densities of the fermion system are represented by

$$n_1 = \frac{n_e}{2N-1} - \frac{n_e}{\beta}, \quad n_2 = \frac{n_e}{2N-1} + \frac{n_e}{\beta}. \tag{72}$$

By utilizing Eq. (70) we find

$$N_1 = \frac{\beta}{2(2N-1)} - \frac{1}{2}, \quad N_2 = -\frac{\beta}{2(2N-1)} - \frac{1}{2}, \tag{73}$$

and substituting this in Eq. (71) we derive the fermion conductivity tensor more accurate than in Eq. (69)

$$\sigma^f_{xx} = \frac{\beta}{2(2N-1)}\frac{e^2}{2\pi\hbar}, \quad \sigma^f_{xy} = -\frac{1}{2}\frac{e^2}{2\pi\hbar}. \tag{74}$$

By following the procedure outlined in Ref. 11 we find the conductivity of the Nth electron Landau level to be

$$\sigma^N_{xx} = \frac{N - 1/2}{\beta}\frac{e^2}{2\pi\hbar}, \quad \sigma^N_{xy} = \frac{1}{2}\frac{e^2}{2\pi\hbar}. \tag{75}$$

By using Eq. (31) we find the conductivity tensor

$$\sigma_{xx} = \frac{N - 1/2}{\beta}\frac{e^2}{2\pi\hbar}, \quad \sigma_{xy} = (N - 1/2)\frac{e^2}{2\pi\hbar}. \tag{76}$$

Thus we see that σ_{xx} scales as the inverse of the magnetic field. Because $\beta \gg 1$ ρ_{xx} at half-integer filling factors scales linearly with the magnetic field.

In the case when $N_1 = 0$ and $N_2 = -1$ in Eq. (73) we have a network consisting of a single fermion edge channel. By going through a standard procedure we find the exact conductivity tensor to be

$$\sigma^N_{xx} = \frac{1}{2}\frac{e^2}{2\pi\hbar}, \quad \sigma^N_{xy} = \frac{1}{2}\frac{e^2}{2\pi\hbar}, \tag{77}$$

in agreement with Eq. (33) which was obtained without considering fermions.

Our derivation was based on a somewhat artificial model in which the effective magnetic field seen by fermions is assumed to vary in a steplike manner assuming only two values ΔB. This could be realized if the incompressible strips on the sides of the compressible transport strip were wide enough.

A more realistic model may be the linear-step model. In this case the magnetic field is assumed to vary linearly between the regions with opposite magnetic field sign. To study this case let us go back to a single channel problem with magnetic field now given by

$$B = \begin{cases} -\Delta B, & y < -d, \\ \Delta B \frac{y}{d}, & |y| < d, \\ \Delta B, & y > d. \end{cases} \tag{78}$$

A similar problem has been considered by Müller.[47] By following the same procedure as for the step model we arrive to the spectrum of the free-particle Hamiltonian with the magnetic field described by Eq. (78) shown in Fig. 9. The new feature is the existence of the edge states at $p_x > 0$. These are the states which cross the Fermi energy in Fig. 9 with $\partial e/\partial p_x > 0$. They come in pairs, corresponding to the two possibilities to be to the left and to the right of $y = 0$. One can see that these states have velocity in the direction opposite to the one of the snake states. Because of this it is necessary to consider backscattering from snake to edge states. Of course, in a translationally invariant magnetic field all the snake and edge states are exact eigenstates, orthogonality of which implies the absence of scattering. We will assume that there exists a small number of short-range scatterers that generate hopping matrix elements.

It seems reasonable to assume that because all the snake states are centered at $y = 0$ they are all coupled to each other. Edge states, on the contrary, are spatially separated and the rate of equilibration may be different between different states. To get an idea of what the real situation might be let us consider the case when all the edge states except the ones corresponding to the lower k Landau levels are coupled to the snake states. Suppose there are N_s channels of snake states, i.e., those with $\partial\epsilon/\partial p_x < 0$ in Fig. 9 (there $N_s = 10$). Then the number of edge channels with $\partial\epsilon/\partial p_x > 0$ which couple to the snake states is $N_s - 2k$ (the factor 2 comes in because of the degeneracy). If the channel is long enough then all but $2k$ channels should backscatter, meaning that the conductance is given by[49]

$$g = 2k\frac{e^2}{2\pi\hbar}. \tag{79}$$

One can see from Eq. (79) that only if we assume that

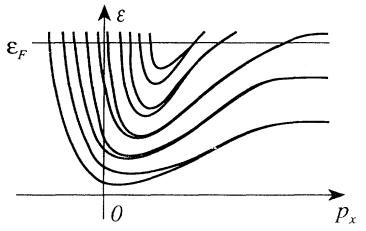

FIG. 9. Spectrum of the free-particle Hamiltonian with the linear-step magnetic field.

all the edge channels are coupled to the snake channels Eq. (68) is recovered. In reality, the lines of zero magnetic field are not straight: they meander in the random potential. This should lead to the scattering between edge channels even in the absence of the short-range disorder. Also, in both models considered so far we had to assume the existence of the insulating regions, where all the states are localized. But in the presence of the scattering, extended states admix to the localized ones. Thus in the limit of strong scattering the network model loses its validity. A more appropriate picture may be that fermion orbits sweep the whole plane, making the concept of channels obsolete. In the following we give a quasiclassical argument which shows that even in this case when all the fermions participate in transport, the result of Eq. (69) holds.

In this case a typical fermion drifts perpendicular to the magnetic field gradient with the velocity[50]

$$v_d \approx v_F^f R_c^f \frac{\nabla B}{B} \approx v_F^f \frac{R_c}{d_s}. \tag{80}$$

A typical fermion changes its direction on a length scale d_s, which we take to be the mean free path. The diffusion constant in this case is given by

$$D \approx d_s v_d \approx v_F^f R_c^f. \tag{81}$$

By making use of the Einstein relation we find the conductivity to be

$$\sigma_{xx}^f \approx k_F^f R_c^f \frac{e^2}{2\pi\hbar}, \tag{82}$$

in agreement with Eq. (69). Of course we cannot obtain a numerical coefficient in this estimate and it is not clear whether it should be the same as in Eq. (69).

VI. COMPOSITE FERMIONS OF HIGHER GENERATIONS

In Sec. IV we have described how the peaks of the longitudinal conductance evolve with varying disorder. It was shown that when the fractional peaks first develop they are in the critical state, meaning that their width should go to zero in the low-temperature limit. Then their magnitude is given by Eqs. (49) and (52). As disorder is reduced the peaks become transitional; their height is reduced from the critical values given in Eqs. (49) and (52). As disorder is reduced further, fractional daughter states develop on the place of each peak in accordance with the phase diagram proposed in Ref. 11. These daughter states are in the same relation to the mother state as the fractions of the main sequence to the integer states.

These states should also be characterized by the universal resistivity values, which may be obtained in the spirit of the Eq. (49) derivation. According to the proposed in Ref. 11 global phase diagram, there is a Fermi-liquid state exactly at the location of the center of the mother peak. We will calculate the conductivity of this state in analogy with what was done for half-integer filling factors in the preceding section.

Let us recall that the idea behind the resistivity calculation for the half-integer filling factors was to attach two flux quanta to the fermions of the topmost Landau level.[11] Then the average effective magnetic field, which acts on the composite fermions is zero. Naturally, the attachment of the flux quanta does not affect the electrons on the lower Landau level. Thus they see only the external magnetic field.

In a Fermi-liquid state with electron filling factor $(2p-1)/(4p)$ the composite fermions are at filling factor $p-1/2$. The longitudinal resistivity of the fermion system arises from the transport of the composite fermions on the topmost p Landau level. In order to calculate this contribution we add two flux quanta of another Chern-Simons gauge field to each of those fermions, see Fig. 10. This field does not act on the composite fermions on the lower Landau levels.

The typical density deviation δn_e is given by Eq. (40). However it would be incorrect to identify δn_e with the typical density deviation δn_p on the p fermion Landau level. The reason being that these additional fermions also carry flux quanta which produce additional effective magnetic field acting on the fermions of the lower $p-1$ Landau levels, Fig. 10. In order to find δn_p we write this effective magnetic field in terms of the additional density

$$\Delta B = -\delta n_e \frac{2ch}{e}. \tag{83}$$

Then the total density deviation due to the fermions on the first $p-1$ Landau levels is

$$\delta n_e - \delta n_p = (p-1)\frac{e\Delta B}{hc} = -2(p-1)\delta n_e. \tag{84}$$

From this we find the density deviation on the p Landau level

$$\delta n_p = (2p-1)\delta n_e. \tag{85}$$

The typical magnetic field acting on the fermions of the topmost Landau level and created by the flux attached to the additional fermions consists of the contributions

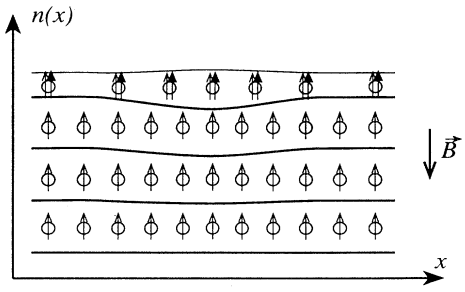

FIG. 10. The composite fermions picture at the electron filling factor 7/16 ($p = 4$). Each arrow represents two flux quanta. Filled-in arrows represent the flux quanta of the field acting only on the fermions belonging to the topmost Landau level. [They will have an opposite direction for the electron filling factor greater than 1/2 ($p < 0$).] The electron density variation results in the decrease in the density on each fermion Landau level except the topmost one.

from two gauge fields and is given by

$$\Delta B' = -\delta n_e \frac{2ch}{e} - (2p-1)\delta n_e \frac{2ch}{e} = -4p\delta n_e \frac{ch}{e}. \quad (86)$$

To calculate the resistivity of the topmost Landau level we can use Eq. (71) which involves the filling factors in the regions of the high and low density N_1, N_2. The two filling factors can be found from Eqs. (85) and (86) to be

$$N_1 = \frac{\frac{n_e}{2p-1} + (2p-1)\delta n_e}{-4p\delta n_e} = -\frac{\beta}{4p(2p-1)} - \frac{2p-1}{4p}, \quad (87)$$

$$N_2 = \frac{\beta}{4p(2p-1)} - \frac{2p-1}{4p}. \quad (88)$$

If N_1 and N_2 become less than 1 it means that the fermion filling factor is not limited to the interval $[p-1, p]$. In this case the compressible liquid occupies only narrow strips and we should use the edge-channel-network model. This condition is close to the one in Eq. (46).

According to Eq. (71) conductivity for the fermions of the second generation is given by

$$\sigma_{xx}^{f'} = \frac{e^2}{2\pi\hbar}\frac{\beta}{4p(2p-1)}, \quad \sigma_{xy}^{f'} = \frac{e^2}{2\pi\hbar}\frac{1}{2}. \quad (89)$$

By going through the sequence of transformations outlined twice in Ref. 11 we can obtain an expression for the physical resistivity from Eq. (89). In the course of transformation we assume that β is the largest parameter in the calculations.

$$\rho_{xx}^{f'} = \frac{2\pi\hbar}{e^2}\frac{4p(2p-1)}{\beta}, \quad \rho_{xy}^{f'} = \frac{2\pi\hbar}{e^2}\frac{[4p(2p-1)]^2}{2(\beta)^2}. \quad (90)$$

By adding the contribution from the Chern-Simons field and inverting the matrix we find

$$\sigma_{xx}^{f} = \frac{e^2}{2\pi\hbar}\frac{4p(2p-1)}{4\beta}, \quad \sigma_{xy}^{f} = \frac{e^2}{2\pi\hbar}(p-\tfrac{1}{2}). \quad (91)$$

By making a transformation to the resistivity tensor and adding the Chern-Simons contribution we get

$$\rho_{xx} = \frac{2\pi\hbar}{e^2}\frac{4p}{\beta(2p-1)}, \quad \rho_{xy} = \frac{2\pi\hbar}{e^2}\frac{-4p}{2p-1}. \quad (92)$$

The same procedure applied to the filling factors larger than 1/2 leads to the conclusion that the longitudinal resistivity is inversely proportional to the filling factor ν for the even-denominator states of the principal sequence

$$\rho_{xx} = \frac{1}{\nu\beta}\frac{2\pi\hbar}{e^2}. \quad (93)$$

At this point we would like to address the question of localization. Although the nature of delocalized states in a strong magnetic field remains unclear, by making the transformation to the composite fermions we can apply the results for localization at zero magnetic field. Strictly speaking, in two dimensions all the states should be localized. However the localization length may be exponentially large, making the effects of localization unobservable. One can see though from Eq. (89) that at sufficiently large p the fermion conductivity is close to $e^2/2\pi\hbar$, making localization length small. The localization should manifest itself in the temperature dependence of the resistivities at even-denominator filling factors. The higher the value of p is, the easier the fermion system can be localized. At low enough temperatures Eq. (93) should only hold for the half-integer filling factors.

It seems possible that transitional peaks correspond to the situation when all the 2DEG planes are occupied by the compressible liquid. Then the high values of the resistivity are due to the localization of the fermion system.

Now we would like to go back and clarify the meaning of the transition from narrow to wide edge channels which yielded the value of p_{c1}. From the consideration of the last two sections one can see that the number of the composite fermion channels depends on the magnetic field gradient which is determined by the electron density distribution.

First, let us consider an integer edge channel. When the channel is extremely narrow the effective magnetic field acting on fermions varies in a steplike manner. Then there is just one fermion Landau level crossing the Fermi level, thus creating a single fermion channel. If the background charge density gradient is reduced the edge channel becomes wider as discussed in Sec. II. The magnetic field gradient becomes smaller and higher Landau levels descend and cross the Fermi level, leading to the appearance of the pairs of snake and edge channels of composite fermions. The total conductance of the integer channel remains the same because of the opposite velocities of the snake and edge channels. However, we run into difficulties with the network model. It was assumed in Sec. III that at the intersection each electron can go right or left with probability 1/2. It is clear now that in the wide edge channels different fermion channels would have different scattering probabilities and the network model is oversimplified.

The same argument for the fractional edge channels of the principal sequence can be carried out by considering the channels of the second generation fermions. This elucidates the significance of p_{c1} found in Sec. IV.

VII. COMPARISON WITH EXPERIMENT

In this section we compare our results with a series of available experimental observations made on extremely high-mobility GaAs heterostructures.

In Sec. IV we predict that the conductivity of the critical fractional peaks is universal, Eq. (52): it only depends on the peak's filling factor. However the comparison with experiment is complicated by the fact that for any given sample only some peaks are critical and it is hard to determine unambiguously which ones. A peak may look critical but, in reality, be on the early stages of transition, thus having a lower than expected conductivity.

When interpreting the experimental results it is useful to realize that according to Eqs. (49) and (52) the particle-hole symmetry is present for the conductivities of the critical peaks, but not for their resistivities. On the other hand, peaks of the principal sequence at filling

factors with the same numerators have the same resistivities.

Extremely helpful for the purpose of verifying the universal values would be an experiment in which the level of disorder is changed continuously. Then the maximum conductivity value achieved by a given peak should approach the universal value. We are aware of only one experiment in which a variation of disorder was attempted. Sajoto *et al.*[45] have studied the FQHE in the GaAs heterostructures, varying the electron density by applying voltage to a back gate. Because of the dependence of screening on the concentration of carriers this results in varying the level of disorder.

We focus on the observations on sample $M73$ presented in Fig. 3 of Ref. 45. Let us follow the behavior of the 3/8 ($p = 2$) peak between the 1/3 and 2/5 states. This peak is still undeveloped at the density $n_e = 1.7 \times 10^{10}$ cm^{-2}; it looks close to critical at $n_e = 2.2 \times 10^{10}$ cm^{-2} and it is transitional at $n_e = 5.0 \times 10^{10}$ cm^{-2}. (A detailed study of the temperature dependence of the peak's shape could probably verify the diagnosis.) Thus the resistivity for this peak is 4 arb. units. The 7/12 ($p = -3$) peak between the 3/5 and 4/7 states is undeveloped at $n_e = 2.2 \times 10^{10}$ cm^{-2} and it is close to critical at $n_e = 5.0 \times 10^{10}$ cm^{-2}. Its resistivity is 1.1 arb. units. The ratio of the resistivities of the two peaks is approximately 3.6. On the other hand, by using Eqs. (50) and (51) this ratio should be 5. This disagreement is probably due to the fact that at $n_e = 2.2 \times 10^{10}$ cm^{-2} the 3/8 peak is already transitional.

The limits of the critical regime are given in Eqs. (46) and (56) in terms of β. However we do not think one can use Eq. (40) in these criteria because of the possible correlations in the distribution of ionized donors. It seems likely that such correlations exist because of the lower than expected values of the resistivity of the Fermi-liquid states, which we discuss next.

Störmer *et al.*,[46] following an earlier conjecture of Chang and Tsui[51] have shown that at relatively high temperature (0.3 K) the longitudinal resistivity is amazingly linear with the exception of dips at the integer and odd-denominator filling factors. They introduced parameter β as a ratio of the classical Hall resistivity to the linear approximation of ρ_{xx}. Explanation of the linear behavior was given in Secs. V and VI in the framework of the composite fermions. We defined β as a microscopic parameter and showed that it enters the expression for ρ_{xx}, Eq. (6) the same way as the phenomenological β of Ref. 46. Therefore we assume our β to be identical to the one introduced by Störmer *et al.*

The value of β was found in Ref. 46 to be almost independent of temperature and to be equal to 23 and 36 for two different samples, while the estimate according to Eq. (40) gives 21 and 9.6 correspondingly. Such a big discrepancy for the higher mobility sample probably implies the importance of correlations in the ionized donor distribution. At lower temperatures[25] resistivity at half-integer is mostly unchanged while at other even-denominator fractions it grows significantly.

The linear dependence of the resistivity at half-integer filling factors can also be seen in the data of Refs. 45 and 53 at very low temperatures. Again at other even-denominator fractions such as 3/8, 1/4, and 3/4 the resistivity seems to grow as temperature is lowered.

As discussed in Sec. VI the Fermi liquid at filling factors with large p can be easily localized. This could serve to explain the deviation of the resistivity from the values given by Eq. (93) at temperatures so low that the inelastic scattering length is larger than the localization length.

The linear dependence of the Fermi-liquid states' resistivity on the magnetic field as described by Eq. (93) makes it possible to extract the value of β from experiment without relying on the assumption of an uncorrelated donor distribution.

Below we give the comparison of our predictions of the universal resistivity values, Eq. (49) with the results of several experimental groups. We would like to emphasize that the presence of the nonlocal transport[43] might have severely affected the measurements.

By analyzing the data of Clark presented in Fig. 2(a) of Ref. 52 we determine that the peaks at filling factors 7/16, 9/20, and 9/16 are critical, while the peak at 7/12 is probably slightly transitional. We find that the resistivities of those peaks agree with Eq. (49) within the accuracy of 15%.

In a recent paper Du *et al.*[25] have reported the observation of the main sequence fractions up to 9/17 and 9/19. From Eq. (93) we find that β is approximately 35. Then according to Eqs. (46) and (56) we have $p_{c1} \approx 4$ and $p_{c2} \approx 8$. It seems that in the data of Ref. 25 peaks at filling factors 9/20, 11/24, and 13/28 ($p = 5, 6, 7$), and 9/16, 11/20, and 13/24 ($p = -4, -5, -6$) are indeed critical. One can see that the resistivity of those peaks does indeed scale in agreement with Eq. (49). However the absolute values given by Eq. (49) are approximately 6 times smaller than the experimental ones.

By analyzing the data of Willett *et al.*,[53] Fig. 1, we determine that the peaks at filling factors 5/12, 7/16, 9/20, and 7/12, 9/16 are critical. Their resistivities scale in agreement with Eq. (49), although the experimental values seem to be 1.5 times larger. We do not have at present any reasonable explanation for the discrepancies in the absolute values.

VIII. CONCLUSIONS

In this paper we presented a unified picture of the dissipative transport between the quantum Hall plateaus for the case of the long-range disorder potential. The basic assumption is the breakup of the electron system into the incompressible regions with integer or fractional filling factors, separated by the network of edge channels. We have considered the structure of edge channels and applied it to the analysis of the transport in the network.

A diverse experimental data on the longitudinal resistivity can be understood by considering the evolution of a single resistivity peak with the variation of disorder, which we describe by a single parameter β. We have shown that each peak goes through four stages in its life: underdevelopment, criticality, transition, and the Fermi-liquid stage. By considering the electrostatics of edge channels, we have found the values of β which determine

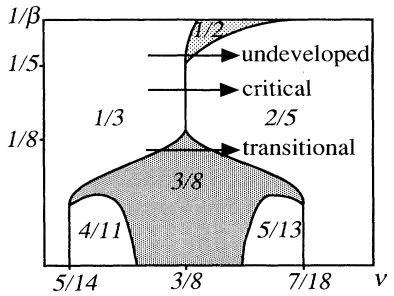

FIG. 11. The fragment of the global phase diagram of the quantum Hall effect. Arrows show trajectories in the $\beta - \nu$ space corresponding to the existing measurements (sweeping magnetic field at constant disorder). The corresponding peak type is indicated.

the beginning and the end of the critical regime.

The evolution of the peak can be understood by considering the global phase diagram of the quantum Hall effect proposed in Ref. 11. We represent disorder by a single parameter β and show the fragment of the phase diagram in Fig. 11. The different kinds of peaks correspond to sweeping magnetic field at different values of β as shown in Fig. 11.

Resistivities of the peaks in the critical regime are given by the universal values, which are in agreement with the law of corresponding states. We have obtained these values by making the transformation to the composite fermions and applying the result for the universal conductivity of the half-filled Landau level to be $1/2(e^2/2\pi\hbar)$. We find that experimentally the relative heights of the critical peaks are in agreement with our prediction, while the absolute values vary from one experimental group to another and are in the worst case several times different. We speculate that this is due to the nonlocal transport contribution. A detailed experimental study of the absolute values possibly using the Corbino geometry or noncontact measurements is clearly desirable.

When the electron density fluctuations are small, compressible liquid occupies the whole plane. In this regime a proper description is given by the Fermi-liquid theory of the composite fermions. Resistivity in this case arises from the fictitious magnetic field fluctuations related to the fluctuations in electron density. We have solved this problem in the case of a steplike variation of the magnetic field by invoking the concept of the snake states. We have found a great similarity between the edge state and the snake state networks and give a general formula for the conductivity tensor of the network.

We have found that the resistivity of the half-integer Fermi-liquid states and of the principal sequence even-denominator fractions is linear in the magnetic field and inversely proportional to β. This conclusion is in agreement with the recent experimental results, although the analysis of the slope shows that a model of noncorrelated donor distribution is oversimplified. We attribute the experimentally observed low-temperature growth of the resistivity at even-denominator principal fractions to the localization of the fermion system.

Note added in proof. Recently, V. Goldman *et al.* have performed conductivity measurements in Corbino geometry. Peak conductivity on some samples is within 30% of universal values. However, other samples give values far from theoretical prediction. At present we do not understand the origin of such discrepancy.

ACKNOWLEDGMENTS

We would like to thank B.I. Halperin for many helpful suggestions throughout the course of this work. We also acknowledge useful discussions with B.L. Altshuler, O. K. K. Lee, L.S. Levitov, K.A. Matveev, P.L. McEuen, I.M. Ruzin, B.I. Shklovskii, and X.G. Wen. We are grateful to the authors of Refs. 24, 25, 28, 36, 38, and 46 for sending us their papers prior to publication. This research was supported by the NSF under Grant No. DMR 89-13624.

APPENDIX A

We have to solve the Laplace equation in the xz plane with the mixed boundary conditions given on the x axis in terms of the electric field:

$$\begin{aligned} &E_x(x,0) = 0 \quad \text{for } |x| > x_2, \\ &E_x(x,0) = 0 \quad \text{for } |x| < x_1, \\ &E_z(x,0) = 2\pi e\left(n'x - \frac{n_L}{2}\right) \quad \text{for } x_1 < x < x_2, \\ &E_z(x,0) = 2\pi e\left(n'x + \frac{n_L}{2}\right) \quad \text{for } -x_2 < x < -x_1. \end{aligned} \tag{A1}$$

Instead we will look for an analytic function $F(\zeta)$ ($\zeta = x + iz$), such that

$$\mathrm{Im}F = E_x, \tag{A2}$$

$$\mathrm{Re}F = E_z. \tag{A3}$$

From Eq. (A1) we know the real and imaginary parts of F on different intervals. However, we have to know the imaginary part of the function on the whole axis in order to determine it in the complex plane. Thus we use another analytic function

$$f = \frac{F}{\sqrt{(\zeta^2 - x_2^2)(\zeta^2 - x_1^2)}}. \tag{A4}$$

By rewriting Eq. (A1) in terms of this function we have

$$\begin{aligned} &\mathrm{Im}f(x,0) = 0 \quad \text{for } |x| > x_2, \\ &\mathrm{Im}f(x,0) = 0 \quad \text{for } |x| < x_1, \\ &\mathrm{Im}f(x,0) = -2\pi e\left(n'x - \frac{n_L}{2}\right)\frac{1}{\sqrt{(x_2^2 - x^2)(x^2 - x_1^2)}} \quad \text{for } x_1 < x < x_2, \\ &\mathrm{Im}f(x,0) = 2\pi e\left(n'x + \frac{n_L}{2}\right)\frac{1}{\sqrt{(x_2^2 - x^2)(x^2 - x_1^2)}} \quad \text{for } -x_2 < x < -x_1. \end{aligned} \tag{A5}$$

The value of f in the complex plane is given by

$$f(\zeta) = \frac{1}{\pi} \int \frac{\mathrm{Im} f(x) dx}{x - \zeta}. \tag{A6}$$

By substituting Eq. (A5) in Eq. (A6) and going back to the electric field we find

$$E_z(x,0) = 4ex \sqrt{\left(1 - \frac{x_2^2}{x^2}\right)\left(1 - \frac{x_1^2}{x^2}\right)} \int_{x_1}^{x_2} \frac{dt(n't - \frac{n_L}{2})}{\sqrt{(x_2^2 - t^2)(t^2 - x_1^2)(1 - \frac{t^2}{x^2})}}. \tag{A7}$$

From the condition that the charge density should be zero at $x \to \infty$ it follows that

$$\int_{x_1}^{x_2} \frac{dx(n'x - \frac{n_L}{2})}{\sqrt{(x_2^2 - x^2)(x^2 - x_1^2)}} = 0. \tag{A8}$$

The second equation follows from the condition that the potential drop between the metal plates is $\Delta\mu/e$:

$$\frac{2\pi e}{\epsilon} \int_{x_1}^{x_2} \frac{dx(n'x - \frac{n_L}{2})}{\sqrt{(x_2^2 - x^2)(x^2 - x_1^2)}} x^2 = \frac{\Delta\mu}{e}. \tag{A9}$$

[1] K. von Klitzing, G. Dorda, and M. Pepper, Phys. Rev. Lett. **45**, 494 (1980).

[2] D.C. Tsui, H.L. Störmer, and A.C. Gossard, Phys. Rev. Lett. **48**, 1559 (1982).

[3] See, e.g., *The Quantum Hall Effect*, edited by R.E. Prange and S.M. Girvin (Springer-Verlag, New York, 1987).

[4] R.B. Laughlin, Phys. Rev. Lett. **50**, 1395 (1983).

[5] R.B. Laughlin, Phys. Rev. B **23**, 5632 (1981); B.I. Halperin, *ibid.* **25**, 2185 (1982).

[6] We do not consider effects related to the formation of the Wigner crystal in this paper.

[7] J. Kucera and P. Streda, J. Phys. C **21**, 4357 (1988).

[8] A. Szafer, A.D. Stone, P.L. McEuen, and B.W. Alphenaar, in *Granular Nanoelectronics*, edited by D.K. Ferry, J.R. Barker, and C. Jacoboni (Plenum, New York, 1991).

[9] J.K. Jain, S.A. Kivelson, and N. Trivedi, Phys. Rev. Lett. **64**, 1297 (1990); **64**, 1993(E) (1990).

[10] S. Kivelson, D.-H. Lee, and S.-C. Zhang, Phys. Rev. B **46**, 2223 (1992); D.-H. Lee, S.A. Kivelson, S.-C. Zhang, Phys. Rev. Lett. **68**, 2386 (1992).

[11] B.I. Halperin, P.A. Lee, and N. Read, Phys. Rev. B **47**, 7312 (1993).

[12] V. Kalmeyer and S.-C. Zhang, Phys. Rev. B **46**, 9889 (1992).

[13] S. Luryi, in *High Magnetic Fields in Semiconductor Physics*, edited by G. Landwehr (Springer, New York, 1987).

[14] A.L. Efros, Solid State Commun. **65**, 1281 (1988).

[15] A.L. Efros, Solid State Commun. **67**, 1019 (1988).

[16] See, e.g., H.P. Wei, S.Y. Lin, D.C. Tsui, and A.M.M. Pruisken, Phys. Rev. B **45**, 3926 (1992), and references therein.

[17] D.B. Chklovskii, B.I. Shklovskii, and L.I. Glazman, Phys. Rev. B **46**, 4026 (1992); **46**, 15 606(E) (1992).

[18] C.W.J. Beenakker, Phys. Rev. Lett. **64**, 216 (1990).

[19] A.M. Chang, Solid State Commun. **74**, 871 (1990).

[20] J.K. Jain, Phys. Rev. Lett. **63**, 199 (1989).

[21] B.E. Kane, Ph.D. thesis, Princeton University, 1988.

[22] A.L. Efros, Phys. Rev. B **45**, 11 354 (1992).

[23] In fact, this equation differs by a factor of 2 from Eq. (20) of Ref. 17 because of the different boundary conditions chosen in this paper [see Eq. (10)]. Factor $2\pi e/\epsilon$ is taken in Eq. (10) in anticipation that the dipolar strip width is smaller than the distance to the surface of the semiconductor.

[24] N.R. Cooper and J.T. Chalker, Phys. Rev. B **48**, 4530 (1993).

[25] R.R. Du, H.L. Störmer, D.C. Tsui, L.N. Pfeiffer, and K.W. West, Phys. Rev. Lett. **70**, 2944 (1993).

[26] T. Chakraborty and P. Pietilainen, *The Fractional Quantum Hall Effect* (Springer-Verlag, New York, 1988).

[27] B.J. van Wees, L.P. Kouwenhoven, E.M.M. Willems, C.J.P.M. Harmans, J.E. Mooij, H. van Houten, C.W.J. Beenakker, J.G. Williamson, and C.T. Foxon, Phys. Rev. B **43**, 12 431 (1991).

[28] B.W. Alphenaar, P.L. McEuen, R.G. Wheeler, and R.N. Sacks, Phys. Rev. Lett. **64**, 677 (1990); B. W. Alphenaar, Ph.D. thesis, Yale University, 1991; B.W. Alphenaar, P.L. McEuen, R.G. Wheeler, and R.N. Sacks (unpublished).

[29] B.J. van Wees, E.M.M. Willems, L.P. Kouwenhoven, C.J.P.M. Harmans, J.G. Williamson, C.T. Foxon, and J.J. Harris, Phys. Rev. B **39**, 8066 (1989).

[30] S. Komiyama, H. Hirai, S. Sasa, and S. Hiyamizu, Phys. Rev. B **40**, 12 566 (1989).

[31] G. Müller, D. Weiss, S. Koch, K. von Klitzing, H. Nickel, W. Schlapp, and R. Lösch, Phys. Rev. B **42**, 7633 (1990).

[32] S. Komiyama and H. Nii, Physica B **184**, 7 (1993).

[33] B. Shapiro, Phys. Rev. B **33**, 8447 (1986).

[34] J.T. Chalker, and P.D. Coddington, J. Phys. C **21**, 2665 (1988).

[35] Y. Huo, R.E. Hetzel, and R.N. Bhatt, Phys. Rev. Lett. **70**, 481 (1993).

[36] I.M. Ruzin, Phys. Rev. B **47**, 15 727 (1993).

[37] J.K. Luo, H. Ohno, K. Matsuzaki, T. Umeda, J. Nakahara, and H. Hasegawa, Phys. Rev. B **40**, 3461 (1989).

[38] F.G. Pikus, and A.L. Efros, Phys. Rev. B **47**, 16 395 (1993).

[39] D.B. Chklovskii, K.A. Matveev, and B.I. Shklovskii, Phys. Rev. B **47**, 12 605 (1993).

[40] V.J. Goldman, J.K. Jain, and M. Shayegan, Phys. Rev. Lett. **65**, 907 (1990).

[41] S.-C. Zhang, Int. J. Mod. Phys. B **6**, 25 (1992).

[42] L.P. Kouwenhoven, B.J. van Wees, N.C. van der Vaart, C.J.P.M. Harmans, C.E. Timmering, and C.T. Foxon, Phys. Rev. Lett. **64**, 685 (1990).

[43]J. K. Wang and V. J. Goldman, Phys. Rev. Lett. **67**, 749 (1991); Phys. Rev. B **45**, 13479 (1992).
[44]A. M. Chang and J.E. Cunningham, Phys. Rev. Lett. **69**, 2114 (1992).
[45]T. Sajoto, Y. W. Suen, L. W. Engel, M. B. Santos, and M. Shayegan, Phys. Rev. B **41**, 8449 (1990).
[46]H.L. Störmer, K.W. Baldwin, L.N. Pfeiffer, and K.W. West, Solid State Commun. **84**, 95 (1992).
[47]J.E. Müller, Phys. Rev. Lett. **68**, 385 (1992).
[48]R. Landauer, IBM J. Res. Dev. **1**, 223 (1957); M. Buttiker, Phys. Rev. Lett. **57**, 1761 (1986).
[49]C. Barnes, B.L. Johnson, and G. Kirczenow, Phys. Rev. Lett. **70**, 1159 (1993).
[50]J.D. Jackson, *Classical Electrodynamics* (Wiley, New York, 1975), p. 585.
[51]A.M. Chang and D.C. Tsui, Solid State Commun. **56**, 153 (1985).
[52]R.G. Clark, Phys. Scr. **T39**, 45 (1991).
[53]R. Willett, J.P. Eisenstein, H.L. Störmer, D.C. Tsui, A.C. Gossard, and J.H. English, Phys. Rev. Lett. **59**, 1776 (1987).